

# Cellular automata connections

Vladimir García-Morales

Departament de Termodinàmica, Universitat de València,  
E-46100 Burjassot, Spain  
garmovla@uv.es

It is shown that any two cellular automata (CA) in rule space can be connected by a continuous path parameterized by a real number  $\kappa \in (0, \infty)$ , each point in the path corresponding to a coupled map lattice (CML). In the limits  $\kappa \rightarrow 0$  and  $\kappa \rightarrow \infty$  the CML becomes each of the two CA entering in the connection. A mean-field, reduced model is obtained from the connection and allows to gain insight in those parameter regimes at intermediate  $\kappa$  where the dynamics is approximately homogeneous within each neighborhood.

Cellular automata (CA) [1–10], coupled map lattices (CML) [11–17] and (nonlinear) partial differential equations [18, 19] constitute the different mathematical approaches to model spatiotemporal pattern formation outside of equilibrium, as found in experimental systems [2]. CAs are fully discrete coupled maps in which space and time are discrete and the local phase space is both discrete and finite. CAs serve as toy models for the overall observed features of complex physical systems [1]. An example of this is spatiotemporal intermittency [1, 20, 21], found in experimental systems [22–28]. However, because of being fully discrete, these models are not realistic: Natural physical systems display a great deal of variability and their evolution departs from the specification of a few rigid, deterministic rules perfectly operating on finite amounts of information. Therefore, it is interesting to study how CAs can be embedded in more sophisticated models, as CMLs [3, 17, 29–38]. In a previous recent work [17], we have presented a general mechanism that allows any CA to be embedded in a CML in terms of a control parameter  $\kappa$  that governs the embedding. When  $\kappa \rightarrow 0$  the CA dynamics is recovered and, otherwise, for  $\kappa$  finite and sufficiently large, a certain degree of ‘fuzziness’ is present.

In this article we show how any two CAs in rule space can be connected by means of a continuous path parameterized by  $\kappa$  so that in the limits  $\kappa \rightarrow 0$  and  $\kappa \rightarrow \infty$  each of the CAs entering in the connection is obtained. We call these limits the CA limits of the CA connection. For any  $\kappa$  finite, a CML is obtained that has traits present in both limits. For intermediate  $\kappa$  values, we derive a mean-field model of the connection that can qualitatively capture many of its dynamical features, as observed in its spatiotemporal evolution. In general, a finite non-vanishing value of the parameter  $\kappa$  weakens the ‘pure’ behavior of the CA limits and we believe that the general concept of CA connections presented here may be useful in, e.g. biophysical models of multicellular ensembles, where variability and network heterogeneity need to be taken into account [39].

We define the alphabet  $\mathcal{A}_p \equiv \{0, 1, \dots, p-1\}$ ,  $p \geq 2$ ,  $p \in \mathbb{N}$ , as the set of integers in the interval  $[0, p-1]$ . We write  $\mathcal{A}_p^N$  for the Cartesian product of  $N$  copies of  $\mathcal{A}_p$ . Let  $x_t^j \in \mathcal{A}_p$  be a dynamical variable at time  $t \in \mathbb{Z}$  and position  $j \in \mathbb{Z}$  on a ring of  $N_s$  sites,  $j \in [0, N_s-1]$  and let  $l, r$  be non-negative integers. A cellular automaton (CA), with rule vector  $(a_0, a_1, \dots, a_{p^{l+r+1}-1})$ ,  $a_n \in \mathcal{A}_p$ ,  $\forall n \in [0, p^{l+r+1}-1]$ , range  $N = l+r+1$  and Wolfram code  $R = \sum_{n=0}^{p^{l+r+1}-1} a_n p^n$ , is a map  $\mathcal{A}_p^{N_s} \rightarrow \mathcal{A}_p^{N_s}$  acting locally at each site  $j$  as  $\mathcal{A}_p^N \rightarrow \mathcal{A}_p$  and synchronously at every  $t$  according to the universal map [7]

$$x_{t+1}^j = \sum_{n=0}^{p^{r+l+1}-1} a_n \mathcal{B} \left( n - \sum_{k=-r}^l p^{k+r} x_t^{j+k}, \frac{1}{2} \right) \quad j = 0, 1, \dots, N_s - 1 \quad (1)$$

where  $j+k = j+k \pmod{N_s}$  and

$$\mathcal{B}(x, y) = \frac{1}{2} \left( \frac{x+y}{|x+y|} - \frac{x-y}{|x-y|} \right) = \begin{cases} \text{sign } y & \text{if } |x| < |y| \\ \frac{\text{sign } y}{2} & \text{if } |x| = |y| \\ 0 & \text{if } |x| > |y| \end{cases} \quad (2)$$

is the  $\mathcal{B}$ -function of the real variables  $x$  and  $y$  [7].

All parameters specifying any CA rule can be given in a compact notation by means of the code  ${}^l R_p^r$  [7]. For example, all 256 Wolfram elementary CA  ${}^1 R_2^1$  are obtained by taking  $p=2$ ,  $l=r=1$  in Eq. (1). Thus, Wolfram rule 30 is denoted by  ${}^1 30_2^1$  and has rule vector  $(a_0, a_1, \dots, a_7) = (0, 1, 1, 1, 1, 0, 0, 0)$ . In general, the coefficients  $a_n$  of any CA can be directly obtained from the Wolfram code  $R$  by means

of the digit function  $\mathbf{d}_p(n, R)$  [10, 40] as

$$a_n = \mathbf{d}_p(n, R) \equiv \left\lfloor \frac{R}{p^n} \right\rfloor - p \left\lfloor \frac{R}{p^{n+1}} \right\rfloor \quad (3)$$

where  $\lfloor \dots \rfloor$  denotes the lower closest integer (floor) function.

Let the real line excluding all half-integer numbers  $(\dots, -\frac{3}{2}, -\frac{1}{2}, \frac{1}{2}, \frac{3}{2}, \dots)$  be denoted by  $\mathbb{R}_{\setminus \mathbb{Z}/2}$ . From the definition of the  $\mathcal{B}$ -function, it is clear that the function  $\mathcal{B}(n - x, \frac{1}{2})$  for  $n \in \mathbb{Z}$  and  $x \in \mathbb{R}_{\setminus \mathbb{Z}/2}$  provides a surjective application  $\mathbb{Z} \times \mathbb{R}_{\setminus \mathbb{Z}/2} \rightarrow \{0, 1\}$ . Thus, if we relax any  $x_t^j$  in Eq. (1) to be a real number so that  $n_t^j \equiv \sum_{k=-r}^l p^{k+r} x_t^{j+k} \in \mathbb{R}_{\setminus \mathbb{Z}/2}$ , we find that  $x_{t+1}^j \in \mathcal{A}_p$ . Therefore, for all initial conditions  $x_0^j$  for which  $n_0^j = \sum_{k=-r}^l p^{k+r} x_0^{j+k} \in \mathbb{R}_{\setminus \mathbb{Z}/2}$  ( $\forall j$ ) the local dynamics provided by Eq. (1) has the form  $\mathcal{A}_p^N \rightarrow \mathcal{A}_p$  for any  $t > 0$ . This fact allowed us to generalize in [17] the universal map for CA, Eq. (1), to real-valued deterministic CA in terms of a  $\kappa$ -deformed function

$$x_{t+1}^j = \sum_{n=0}^{p^{r+l+1}-1} a_n \mathcal{B}_\kappa \left( n - \sum_{k=-r}^l p^{k+r} x_t^{j+k}, \frac{1}{2} \right) \quad j = 0, 1, \dots, N_s - 1 \quad (4)$$

where

$$\mathcal{B}_\kappa(x, y) \equiv \frac{1}{2} \left( \tanh \left( \frac{x+y}{\kappa} \right) - \tanh \left( \frac{x-y}{\kappa} \right) \right) \quad (5)$$

For all finite values of the real variables  $x$  and  $y$ , the  $\mathcal{B}_\kappa$ -function satisfies the limits [17]:

$$\lim_{\kappa \rightarrow \infty} \mathcal{B}_\kappa(x, y) = 0 \quad \lim_{\kappa \rightarrow \infty} \frac{\mathcal{B}_\kappa(x, y)}{\mathcal{B}_\kappa(0, y)} = 1 \quad (6)$$

$$\lim_{\kappa \rightarrow 0} \mathcal{B}_\kappa(x, y) = \mathcal{B}(x, y) \quad \lim_{\kappa \rightarrow 0} \mathcal{B}_\kappa(0, y) = \text{sign } y \quad (7)$$

We also note that  $0 \leq |\mathcal{B}_\kappa(x, y)| \leq 1$ .

Therefore, by using Eq. (7), Eq. (4) becomes equal to Eq. (1) in the limit  $\kappa \rightarrow 0$ . In the limit  $\kappa \rightarrow \infty$  one has, instead  $x_{t+1}^j \sim \frac{1}{2\kappa}$  [17] so that, if the limit is strictly taken  $x_t^j = 0, \forall j$  and  $\forall t > 0$ . We note that, if instead of Eq. (4) we take

$$x_{t+1}^j = \sum_{n=0}^{p^{r+l+1}-1} a_n \frac{\mathcal{B}_\kappa \left( n - \sum_{k=-r}^l p^{k+r} x_t^{j+k}, \frac{1}{2} \right)}{\mathcal{B}_\kappa \left( 0, \frac{1}{2} \right)} \quad j = 0, 1, \dots, N_s - 1 \quad (8)$$

the limit  $\kappa \rightarrow 0$  is as before but now the limit  $\kappa \rightarrow \infty$  is

$$x_{t+1}^j = \sum_{n=0}^{p^{r+l+1}-1} a_n \quad j = 0, 1, \dots, N_s - 1 \quad (9)$$

because of Eq. (6).

The question now arises whether we can modify Eq. (8) so that the limit  $\kappa \rightarrow \infty$  is another cellular automaton of the form of Eq. (1) for all initial conditions  $x_0^j \in \mathcal{A}_p$  ( $\forall j$ ) but with a generally different rule vector  $(b_0, b_1, \dots, b_{p^{l+r+1}-1}), b_n \in \mathbb{Z} \in \mathcal{A}_p, \forall n \in [0, p^{l+r+1} - 1]$

$$x_{t+1}^j = \sum_{n=0}^{p^{r+l+1}-1} b_n \mathcal{B} \left( n - \sum_{k=-r}^l p^{k+r} x_t^{j+k}, \frac{1}{2} \right) \quad j = 0, 1, \dots, N_s - 1 \quad (10)$$

There are, of course, many possibilities for a  $\kappa$ -deformed formula to connect two CA in the limits  $\kappa \rightarrow 0$  and  $\kappa \rightarrow \infty$ . A simple example is given by

$$x_{t+1}^j = \sum_{n=0}^{p^{r+l+1}-1} \left[ a_n \mathcal{B} \left( n - \sum_{k=-r}^l p^{k+r} x_t^{j+k}, \frac{1}{2} \right) \mathcal{B}_\kappa \left( 0, \frac{1}{2} \right) + b_n \mathcal{B} \left( n - \sum_{k=-r}^l p^{k+r} x_t^{j+k}, \frac{1}{2} \right) \mathcal{B}_{1/\kappa} \left( 0, \frac{1}{2} \right) \right] \quad j = 0, 1, \dots, N_s - 1 \quad (11)$$

Eq. (1) is obtained in the limit  $\kappa \rightarrow 0$  of Eq. (11), while Eq. (10) is obtained in the limit  $\kappa \rightarrow \infty$  of Eq. (11). We see that for any value of  $\kappa$ , the time evolution of Eq. (11) is contained in the interval  $[0, 2(p-1)]$ . This means that for  $p = 2$  (Boolean CA in the CA limits), we have  $x_{t+1}^j \in [0, 2]$ .

In this work we consider a  $\kappa$ -deformed formula so that two CA can be connected in the limits  $\kappa \rightarrow 0$  and  $\kappa \rightarrow \infty$  and such that for  $p = 2$  the dynamics is contained in the unit interval,  $x_t^j \in [0, 1]$ ,  $\forall t, j$ . For two CA  ${}^l[R_1]_p^r$  and  ${}^l[R_2]_p^r$ , we define a CA connection, and denote it by  ${}^l[R_1]_p^r \xrightarrow{\kappa} {}^l[R_2]_p^r$  by the map

$$x_{t+1}^j = \sum_{m=0}^{p-1} m \frac{\mathcal{B}_\kappa \left( m - a_t^j(\kappa), \frac{1}{2} \right) \mathcal{B}_{1/\kappa} \left( m - b_t^j(\kappa), \frac{1}{2} \right)}{\mathcal{B}_\kappa(0, \frac{1}{2}) \mathcal{B}_{1/\kappa}(0, \frac{1}{2})} \quad j = 0, 1, \dots, N_s - 1 \quad (12)$$

where

$$a_t^j(\kappa) \equiv \sum_{n=0}^{p^{l+r+1}-1} a_n \mathcal{B}_\kappa \left( n - \sum_{k=-r}^l p^{k+r} x_t^{j+k}, \frac{1}{2} \right) \quad (13)$$

$$b_t^j(\kappa) \equiv \sum_{n=0}^{p^{l+r+1}-1} b_n \mathcal{B}_{1/\kappa} \left( n - \sum_{k=-r}^l p^{k+r} x_t^{j+k}, \frac{1}{2} \right) \quad (14)$$

In the limit  $\kappa \rightarrow 0$ , Eq. (12) becomes Eq. (1) since

$$x_{t+1}^j = \sum_{m=0}^{p-1} m \mathcal{B} \left( m - a_t^j(0), \frac{1}{2} \right) = a_t^j(0) = \sum_{n=0}^{p^{l+r+1}-1} a_n \mathcal{B} \left( n - \sum_{k=-r}^l p^{k+r} x_t^{j+k}, \frac{1}{2} \right) \quad (15)$$

However, in the limit  $\kappa \rightarrow \infty$  Eq. (12) becomes Eq. (10)

$$x_{t+1}^j = \sum_{m=0}^{p-1} m \mathcal{B} \left( m - b_t^j(\infty), \frac{1}{2} \right) = b_t^j(\infty) = \sum_{n=0}^{p^{l+r+1}-1} b_n \mathcal{B} \left( n - \sum_{k=-r}^l p^{k+r} x_t^{j+k}, \frac{1}{2} \right) \quad (16)$$

We note that the transformation  $\kappa \rightarrow 1/\kappa$  merely reverses the connection, i.e.  ${}^l[R_1]_p^r \xrightarrow{\kappa} {}^l[R_2]_p^r$  changes to  ${}^l[R_2]_p^r \xrightarrow{\kappa} {}^l[R_1]_p^r$ .

To get insight in the complex spatiotemporal dynamics of Eq. (12) it proves useful to consider the mean field model obtained by taking  $x_t^j \equiv u_t$ . Then Eq. (12) reduces to

$$u_{t+1} = \sum_{m=0}^{p-1} m \frac{\mathcal{B}_\kappa \left( m - a_t(\kappa), \frac{1}{2} \right) \mathcal{B}_{1/\kappa} \left( m - b_t(\kappa), \frac{1}{2} \right)}{\mathcal{B}_\kappa(0, \frac{1}{2}) \mathcal{B}_{1/\kappa}(0, \frac{1}{2})} \quad (17)$$

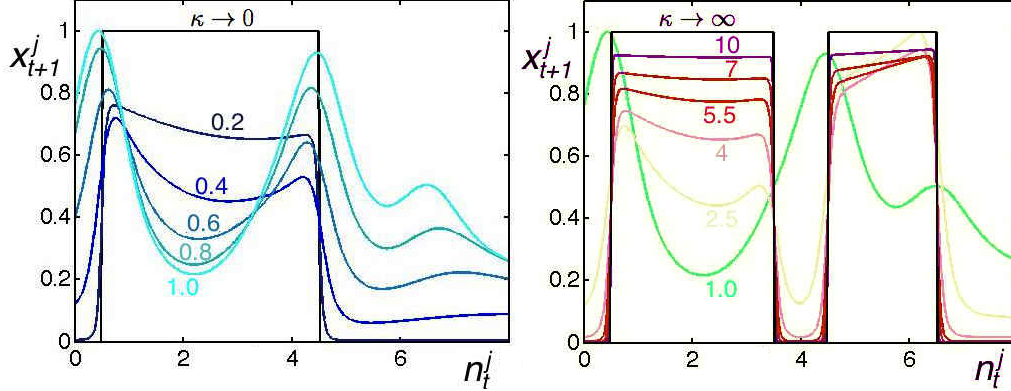


FIG. 1: The cell state  $x_{t+1}^j \in [0, 1]$  vs. the neighborhood sum value  $n_t^j = \sum_{k=-1}^1 2^{k+r} x_t^{j+k}$  for the CA connection  ${}^130_2^1 \xrightarrow{\kappa} {}^1110_2^1$  and for the values of  $\kappa$  indicated on the curves. The panels are separated to better show the changes obtained in Eq. (20) with increasing  $\kappa$  values.

where

$$a_t(\kappa) \equiv \sum_{n=0}^{p^{l+r+1}-1} a_n \mathcal{B}_\kappa \left( n - \frac{p^{l+r+1}-1}{p-1} u_t, \frac{1}{2} \right) \quad (18)$$

$$b_t(\kappa) \equiv \sum_{n=0}^{p^{l+r+1}-1} b_n \mathcal{B}_{1/\kappa} \left( n - \frac{p^{l+r+1}-1}{p-1} u_t, \frac{1}{2} \right) \quad (19)$$

This reduced model describes the behavior of homogeneous initial conditions and is also a mean field approximation for arbitrary (inhomogeneous) initial conditions. Of special interest are the  $\omega$ -limit sets of Eq. (17) and their change with the control parameter  $\kappa$ . These yield the bifurcation diagram of the reduced model that can be used to interpret certain results obtained with the full model.

We note that for Boolean CA connections  $p = 2$ , Eq. (12) simplifies to

$$x_{t+1}^j = \frac{\mathcal{B}_\kappa \left( 1 - a_t^j(\kappa), \frac{1}{2} \right) \mathcal{B}_{1/\kappa} \left( 1 - b_t^j(\kappa), \frac{1}{2} \right)}{\mathcal{B}_\kappa(0, \frac{1}{2}) \mathcal{B}_{1/\kappa}(0, \frac{1}{2})} \quad j = 0, 1, \dots, N_s - 1 \quad (20)$$

and, by the definition of the  $\mathcal{B}_\kappa$  function we find that  $0 \leq x_t^j \leq 1$  for all  $\kappa$ ,  $t$  and  $j$ .

As an example to illustrate the above concepts, we consider a CA connection between the two elementary CA provided by the Boolean CA rules  ${}^130_2^1$  and  ${}^1110_2^1$ . The former one is known to be a random number generator [1, 41] and the second one is capable of universal computation [1, 42]. We thus consider the CA connection  ${}^130_2^1 \xrightarrow{\kappa} {}^1110_2^1$  described by Eq. (20) with  $p = 2$ ,  $l = r = 1$  and rule vectors  $(a_0, a_1, \dots, a_7) = (0, 1, 1, 1, 1, 0, 0, 0)$  and  $(b_0, b_1, \dots, b_7) = (0, 1, 1, 1, 0, 1, 1, 0)$ . Fig. 1 shows  $x_{t+1}^j$  in Eq. (20) as a function of the neighborhood value  $n_t^j = \sum_{k=-1}^1 p^{k+r} x_t^{j+k}$  for different values of  $\kappa$  and for the above CA connection: Note that CA rule  ${}^130_2^1$  is obtained in the limit  $\kappa \rightarrow 0$  (Fig. 1 left) while rule  ${}^1110_2^1$  is obtained in the limit  $\kappa \rightarrow \infty$  (Fig. 1 right). For intermediate values of  $\kappa$  the curves always lie within the unit interval.

The spatiotemporal evolution of  $x_t^j$  obtained from Eq. (20) for the CA connection  ${}^130_2^1 \xrightarrow{\kappa} {}^1110_2^1$  is shown in Fig. 2  $j \in [0, 239]$ ,  $t \in [0, 239]$  and for different  $\kappa$  values indicated over the panels for a simple initial condition consisting of a single site with value '1' surrounded by sites with value '0'.

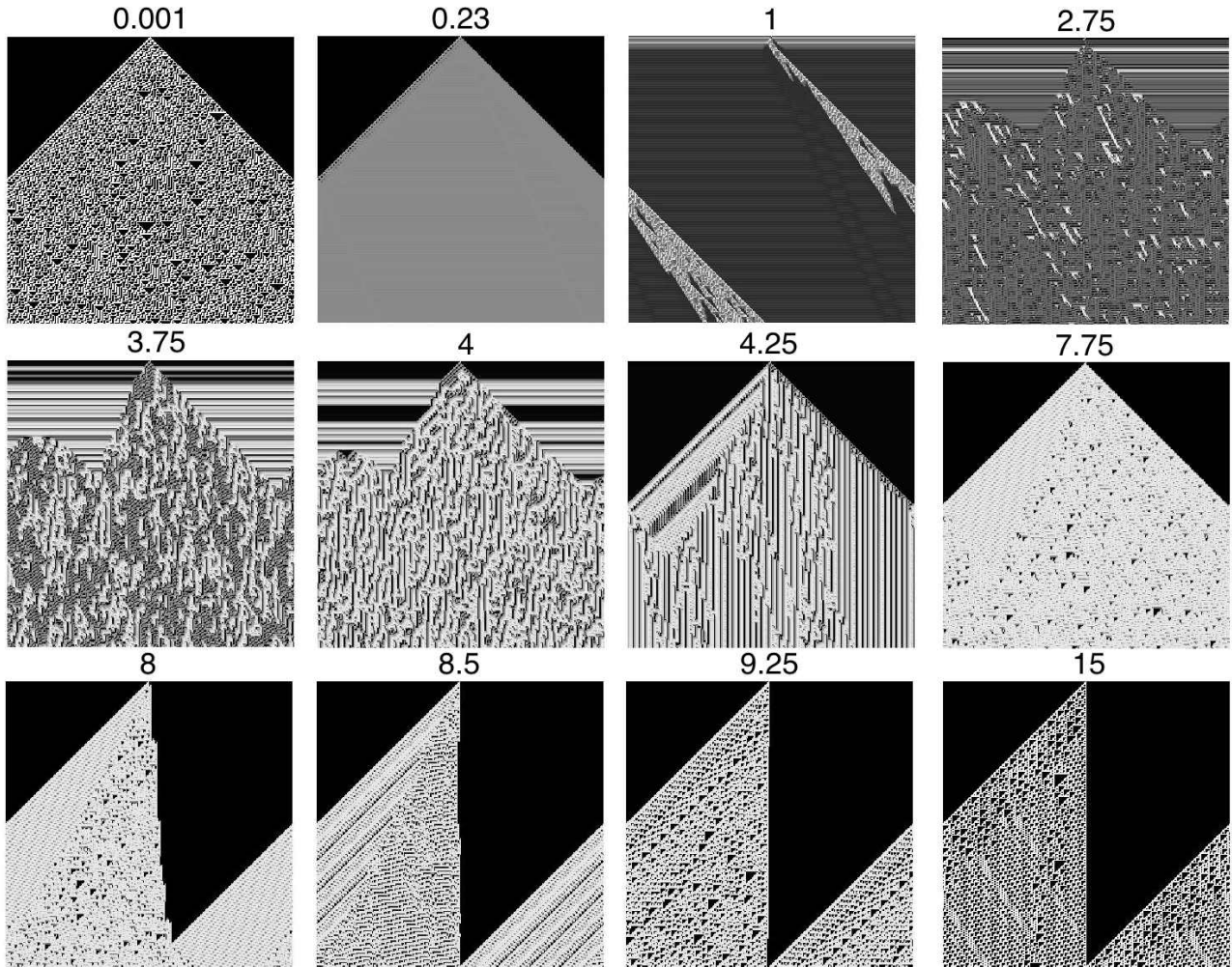


FIG. 2: Spatiotemporal evolution of  $x_t^j$  obtained from Eq. (20) for the CA connection  ${}^130\frac{1}{2} \xrightarrow{\kappa} {}^1110\frac{1}{2}$  starting from a single site with value 1 surrounded by sites with zero value and for the values of  $\kappa$  indicated on the panels. In each panel, time flows from top to bottom. The system size is  $N_s = 240$  and 240 iteration steps are shown. In the gray scale used, black and white correspond to values zero and one, respectively.

For  $\kappa = 0.001$  the behavior typical of the limit  $\kappa \rightarrow 0$  is already observed and the CA connection coincides with Wolfram's CA rule 30. For  $\kappa = 15$  the limit  $\kappa \rightarrow \infty$  is already well approximated and the CA connection coincides with Wolfram's CA rule 110. For intermediate values of  $\kappa$  the behavior is highly nontrivial and gliders and coherent structures typical of Class 4 CA [1, 4] are observed (e.g. for  $\kappa = 4.25$ ). The overall behavior for  $\kappa$  finite somehow interpolates between the limits  $\kappa \rightarrow 0$  and  $\kappa \rightarrow \infty$ , although there is a wide variety of qualitatively different behavior. At  $\kappa = 1$  a coexistence is observed between a traveling turbulent patch at high values of  $x_t^j$  and homogeneous period-2 oscillations that form domains (clusters) connecting two different low values of  $x_t^j$ . Most remarkably, it is observed that in the interval  $2.75 \lesssim \kappa \lesssim 4$ , the homogeneous quiescent state loses stability to aperiodic oscillations, the system being highly sensitive to small perturbations.

Insight on the results of Fig. 2 can be gained by means of the mean-field reduction of the CA

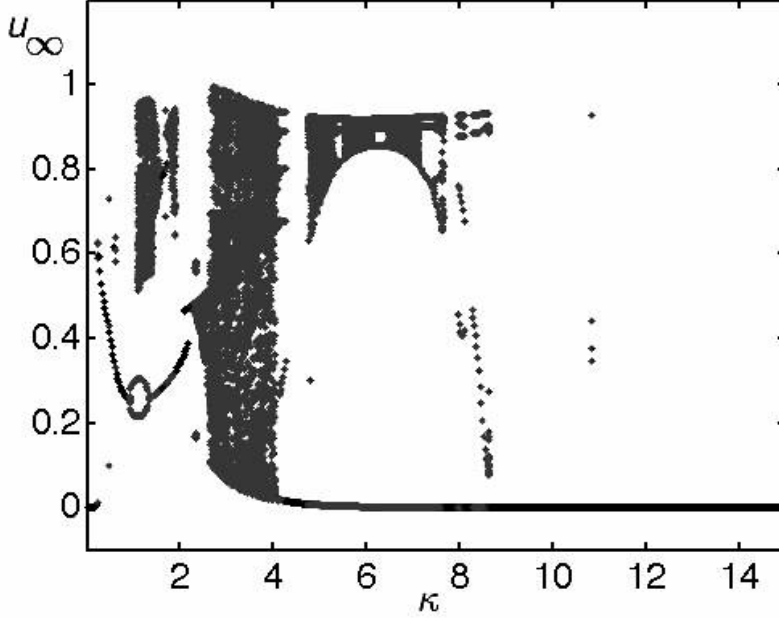


FIG. 3: Bifurcation diagram calculated from the asymptotic behavior of Eq. (21) for the CA connection  ${}^130_2^1 \xrightarrow{\kappa} {}^1110_2^1$ . The values that the dynamical variable  $u_\infty$  takes on the orbit at large times are shown as a function of the parameter  $\kappa$ .

connection, Eq. (17) which, in this particular case, takes the form

$$u_{t+1} = \frac{\mathcal{B}_\kappa(1 - a_t(\kappa), \frac{1}{2})}{\mathcal{B}_\kappa(0, \frac{1}{2})} \frac{\mathcal{B}_{1/\kappa}(1 - b_t(\kappa), \frac{1}{2})}{\mathcal{B}_{1/\kappa}(0, \frac{1}{2})} \quad (21)$$

where

$$a_t(\kappa) \equiv \sum_{n=0}^7 a_n \mathcal{B}_\kappa\left(n - 7u_t, \frac{1}{2}\right) \quad (22)$$

$$b_t(\kappa) \equiv \sum_{n=0}^7 b_n \mathcal{B}_{1/\kappa}\left(n - 7u_t, \frac{1}{2}\right) \quad (23)$$

with  $(a_0, a_1, \dots, a_7) = (0, 1, 1, 1, 1, 0, 0, 0)$  and  $(b_0, b_1, \dots, b_7) = (0, 1, 1, 1, 0, 1, 1, 0)$ .

The bifurcation diagram can be readily calculated by iterating Eq. (21) for sufficiently long times, starting from initial conditions  $u_0 \in [0, 1]$  uniformly filling the unit interval. In this way, the  $\omega$ -limit sets  $u_\infty$  of the values of  $u_t$  as  $t \rightarrow \infty$  are numerically obtained. The bifurcation diagram is shown in Fig. 3 in which  $u_\infty$  is plotted vs.  $\kappa$ .

The observations made in Fig. 2 can be understood by means of the bifurcation diagram in Fig. 3:

- In the limits  $\kappa \rightarrow 0$  and  $\kappa \rightarrow \infty$  we have  $u_\infty \rightarrow 0$ . This corresponds to the CA limits and both rules  ${}^130_2^1$  and  ${}^1110_2^1$  in the connection fix the quiescent state and no other homogeneous configuration. The mean-field model is not able to capture the complex dynamics of Eq. (20) in these CA limits because the dynamical behavior is highly correlated through the CA dynamics and the correlations, that are affected by the neighborhood configurations, are lost in the mean-field model.

- For  $\kappa \approx 1$  the coexistence between two alternating period-2 branches at low values of  $u_\infty$  and a chaotic stripe at high values of  $u_\infty$  is observed. A gap in  $u_\infty$  is seen separating both behaviors. This qualitatively captures the observation made in Fig. 2 for this value of  $\kappa$ .
- In the interval  $2.75 \lesssim \kappa \lesssim 4$ ,  $u_\infty$  displays a wide variety of possible states that are all reached in an aperiodic, chaotic, manner. The branch at low  $u_\infty$  is now fused with the chaotic stripe and there is no gap. This matches the observation made on the turbulent behavior described in Fig. 2 and the mean-field model allows to relate that turbulence in the full model to low-dimensional chaos in the reduced one.
- In the interval  $5 \lesssim \kappa \lesssim 8$  there is a coexistence between stable homogeneous neighborhoods (branch with low  $u_\infty$ ) and a chaotic stripe at high values of  $u_\infty$ . Again, these behaviors are separated by a wide gap in the possible values of  $u_\infty$ .

In this article we have introduced the concept of CA connections. In brief CA connections are CMLs that depend on a control parameter  $\kappa$  such that in the limits  $\kappa \rightarrow 0$  and  $\kappa \rightarrow \infty$  the CML collapses to a CA. We have shown that any two CAs in rule space can be connected in this way. A mean-field, reduced model allows a bifurcation diagram to be calculated that qualitatively captures the features observed in the spatiotemporal evolution of the connection (in those parameter regimes where the neighborhood dynamics is approximately homogeneous). We have illustrated these general results with the specific example of Wolfram elementary Boolean CA rules 30 and 110 [1] constructing a connection between both rules. At intermediate  $\kappa$  values, a wide variety of dynamical behavior has been observed ranging from coherent to seemingly chaotic behavior, as well as the coexistence of coherence and disorder for simple initial conditions. These behaviors have been qualitatively investigated by means of a mean-field model derived from the connection. The results presented in this article can be easily generalized to more dimensions and arbitrary order in time [7].

We note that  $\kappa$  should have a wide physical significance [39]. If one considers physical models of networks governed by a finite set of strict rules, a non-vanishing value for the parameter  $\kappa$  may incorporate the overall effect of the network heterogeneity, as well as the weakening of cooperative phenomena present in the CA limits. If  $\kappa$  is made explicitly dependent on time, the CA connection presented here may also account for the effect of aging in the evolution of a system dynamics.

- 
- [1] S. Wolfram, *A New Kind of Science* (Wolfram Media Inc., Champaign, IL, 2002).
  - [2] A. Deutsch and S. Dormann, *Cellular Automaton Modeling of Biological Pattern Formation: Characterization, Applications, and Analysis* (Birkhäuser, Boston, MA, 2005).
  - [3] T. Tokihiro, D. Takahashi, J. Matsukidaira, and J. Satsuma, Phys. Rev. Lett. **76**, 3247 (1996).
  - [4] A. Ilachinski, *Cellular Automata: a Discrete Universe* (World Scientific, Singapore, 2001).
  - [5] A. Adamatzky, *Identification of Cellular Automata* (Taylor and Francis, London, 1994).
  - [6] A. Wuensche and M. Lesser, *The Global Dynamics of Cellular Automata* (Addison-Wesley, Reading, MA, 1992).
  - [7] V. García-Morales, Phys. Lett. A **376**, 2645 (2012).
  - [8] V. García-Morales, Phys. Lett. A **377**, 276 (2013).



- [9] V. García-Morales, Phys. Rev. E **88**, 042814 (2013).
- [10] V. García-Morales, Nonlinear Sci. Numer. Simulat. **39**, 81 (2016).
- [11] K. Kaneko, Prog. Theor. Phys. **72**, 480 (1984).
- [12] K. Kaneko, Prog. Theor. Phys. **74**, 1033 (1985).
- [13] I. Waller and R. Kapral, Phys. Rev. A **30**, 2047 (1984).
- [14] K. Kaneko, editor, *Theory and Applications of Coupled Map Lattices* (Wiley, New York, 1993).
- [15] L. A. Bunimovich and D. Turaev, Nonlinearity **11**, 1539 (1998).
- [16] L. A. Bunimovich and Y. G. Sinai, Nonlinearity **1**, 491 (1988).
- [17] V. Garcia-Morales, J. Phys. A.: Math. Theor. **49**, 295101 (2016).
- [18] M. C. Cross and P. C. Hohenberg, Rev. Mod. Phys. **65**, 851 (1993).
- [19] Y. Kuramoto, *Chemical Oscillations, Waves and Turbulence* (Springer, New York, 1984).
- [20] Z. Jabeen and N. Gupte, Physica A **384**, 59 (2007).
- [21] Z. Jabeen and N. Gupte, Phys. Lett. A **374**, 4488 (2010).
- [22] S. Ciliberto and P. Bigazzi, Phys. Rev. Lett. **60**, 286 (1988).
- [23] F. Daviaud, M. Dubois, and P. Berge, Europhys. Lett. **9**, 441 (1989).
- [24] S. Bottin, F. Daviaud, O. Dauchot, and P. Manneville, Europhys. Lett. **43**, 171 (1998).
- [25] M. Degen, I. Mutabazi, and C. Andereck, Phys. Rev. E **53**, 3495 (1996).
- [26] G. Colovas and C. Andereck, Phys. Rev. E **55**, 2736 (1997).
- [27] A. Goharzadeh and I. Mutabazi, Eur. Phys. J. B **19**, 157 (2001).
- [28] S. Michalland, M. Rabaud, and Y. Couder, Europhys. Lett. **22**, 17 (1993).
- [29] H. Chate and P. Manneville, Europhys. Lett. **6**, 591 (1988).
- [30] H. Chate and P. Manneville, J. Stat. Phys. **56**, 357 (1989).
- [31] H. Chate and P. Manneville, Physica D **45**, 122 (1990).
- [32] T. Tokihiro, A. Nagai, and J. Satsuma, Inverse Problems **15**, 1639 (1999).
- [33] T. Tokihiro, D. Takahashi, and J. Matsukidaira, J. Phys. A: Math. Gen. **33**, 607 (2000).
- [34] A. Nobe, J. Satsuma, and T. Tokihiro, J. Phys. A: Math. Gen. **34**, L371 (2001).
- [35] M. Białecki and A. Doliwa, Commun. Math. Phys. **253**, 157 (2005).
- [36] M. Białecki, Glasgow Math. J. **47A**, 33 (2005).
- [37] F. Bagnoli and R. Rechtman, Phys. Rev. E, **73**, 026202 (2006).
- [38] W. Just, Phys. Rev. E **74**, 046209 (2006)
- [39] V. García-Morales, J. A. Manzanares and S. Mafe, arXiv:1612.05006 [physics.bio-ph] (2016), submitted.
- [40] V. García-Morales, Chaos Sol. Fract. **83**, 27 (2016).
- [41] S. Wolfram, Phys. Rev. Lett. **55**, 449 (1985).
- [42] M. Cook, Complex Systems, **15**, 1 (2004).